

# 21. The Motor Extended Kalman Filter for Dynamic Rigid Motion Estimation from Line Observations\*

Yiwen Zhang, Gerald Sommer, and  
Eduardo Bayro-Corrochano

Institute of Computer Science and Applied Mathematics,  
Christian-Albrechts-University of Kiel

## 21.1 Introduction

The motion estimation of a moving object in front of an observer is fundamental for various tasks in visual robotics like tracking, object collision avoidance, surveillance and visual navigation.

The issue we are here interested in is the estimation of the rigid motion of an object in observer frame or equivalently, the motion of an observer in a world frame. Fig. 21.1 gives a more detailed illustration. The 3-D coordinate frame  $A$  is supposed as observer frame, the coordinate frame  $B$  is fixed on a moving rigid body. The position and orientation of the rigid body in frame  $A$  are sampled by the observer at discrete time  $t_i$ ,  $i = 0, 1, \dots$ . At time  $t_0$ , frame  $A$  and frame  $B$  are duplicate. At time  $t_i$ , frame  $B$  goes to  $B_i$ , and an observed feature  $L$  on the surface of the rigid body goes to  $L_i$  with respect to frame  $A$ . We use state vector  $\mathbf{X}_i$  to describe the position and orientation of the coordinate frame  $B_i$  relative to the frame  $A$ .  $\mathbf{X}_i$  satisfies the dynamic model (which is also known as the plant model)

---

\* This work has been supported by DFG Grants So-320-2-1, So-320-2-2, and Graduiertenkolleg No. 357.

$$\mathbf{X}_i = \Phi_{i/i-1}(\mathbf{X}_{i-1}, \mathbf{W}_i), \tag{21.1}$$

where  $\mathbf{W}_i$  is independent normally distributed noise with zero mean and known statistics. We will assume that the measurement of the feature  $\mathbf{L}_i$  is also corrupted by independent normally distributed noise  $\mathbf{V}_i$ , which is also zero mean and with known statistics, and it is uncorrelated with  $\mathbf{W}_i$ . The real observed measurement  $\mathbf{L}_i$  is expressed as

$$\mathbf{L}_i = \mathbf{L}'_i + \mathbf{V}_i. \tag{21.2}$$

where  $\mathbf{L}'_i$  are the accurate data. The relationship between the measurements and the state is given by the measurement model as

$$f(\mathbf{L}_0, \mathbf{L}_i, \mathbf{X}_i, \mathbf{V}_0, \mathbf{V}_i) = \mathbf{0}. \tag{21.3}$$

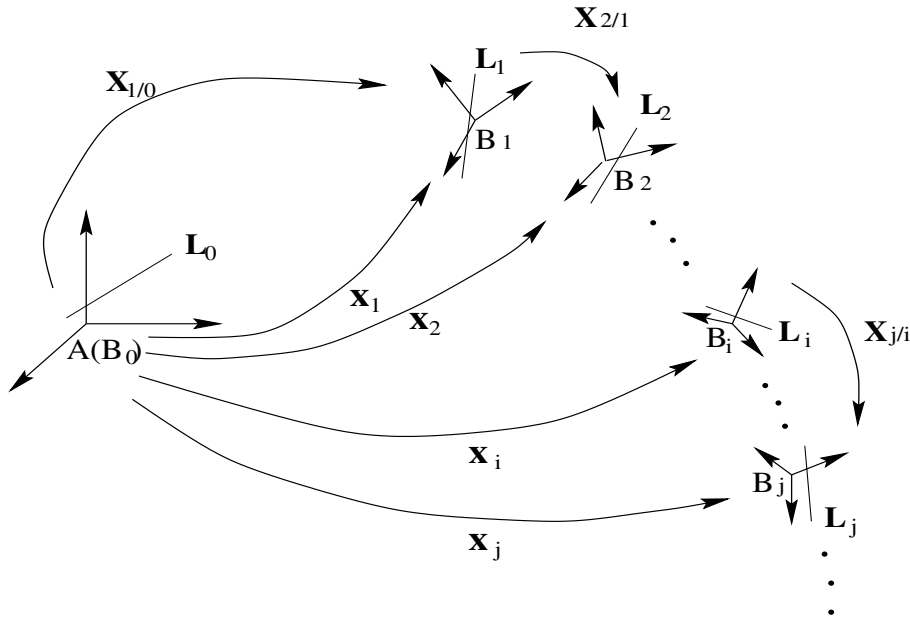


Fig. 21.1. Coordinate frames for observation of rigid motions

In such a noisy scenario we urgently require a method able to estimate a “best” state variable vector  $\hat{\mathbf{X}}_i$ .

The basic 3-D geometric primitives of the visual space for the motion registration are points (corners) or lines (edges). These local features are sensitive to noise and quantization errors which jeopardize to some extent the motion estimation. Alternatively the use of global features such as planes or surfaces makes the motion estimation process more robust, however with higher computational complexity.

In the literature we distinguish basically two main groups of estimation methods: batch and sequential processing.

The batch approaches include SVD and the analytical solutions by minimization techniques in terms of least square error. They use all the features' measurements observed at time  $t_i$  and  $t_j$  to estimate the optimal motion parameters  $\mathbf{X}_{j/i}$  (so called two-view motion parameters) [123] [8] [201]. These batch methods do not use *a priori* information given by (21.1).

The sequential processing scheme is also called Kalman filtering [126] [170] [225]. The state  $\mathbf{X}_i$  is estimated from the current predicted *a priori* state (using (21.1)) and the current measurements. The Kalman filter is a recursive algorithm: the new solution is based on the new measurements and the old solution. If the model equations (21.1) and (21.3) are nonlinear, the extended Kalman filter (EKF) can be used. In computer vision the measurement models are usually nonlinear. For applying the extended Kalman filter, such nonlinear models must be linearized about the current observations and current predicted state.

Former research shows that when we use both the batch and EKF algorithms to estimate the motion parameters with the same given measurements, the later gains better estimates [247]. This results from the use of additional *a priori* information of the dynamic model (21.1) in case of Kalman filter processing. In other words, Kalman filtering is the best solution to our problem stated above.

The application of the Kalman filter as a recursive minimum variance estimator has become popular since the sixties. In order to estimate dynamic motion parameters, authors used the Kalman filter together with different types of state variable representations. For instance, Bar-Itzhack et al. used point sets for the quaternion EKF to estimate dynamic rotation [13] and Zhang and Faugeras used line segments with their midpoints to estimate all dynamic motion parameters with a standard EKF [247]. Recently Azarbayejani and Pentland [11] applied the EKF for estimation of motion and structure using relative orientation constraints in terms of quaternions. These methods are all based on point measurements (a line segment is defined by its midpoint and direction). We have not yet seen a method using straight line measurements.

With recently developed Hough transformation techniques [149], [186] one can extract a 2-D straight line from the image of the object boundary and then reconstruct a 3-D straight line by calibrated images. The coordinates of 3-D reconstructed straight lines are more reliable than 3-D reconstructed points. This motivated us to develop a Kalman filter from straight lines observations.

In this paper, we present the development of a novel EKF in the geometric algebra framework. The key for the filter design is that the measurement model of straight lines is established in the geometric algebra  $\mathcal{G}_{3,0,1}^+$  called motor algebra, which is of the homogeneously extended Euclidean space  $E_3$ .

This aims at the useful property that the nonlinear motion model of a straight line in space  $E_3$  can be written linearly in motor algebra. The modeling of the problem at hand in algebra  $\mathcal{G}_{3,0,1}^+$  corresponds to the implicit assumption of a line geometry. That means that lines are the basic primitive entities (instead of points in  $E_3$ ) and the known approaches of Kalman filter can be used in this algebraic framework. The real experiments show that the motor extended Kalman filter (MEKF) is indeed an attractive estimation approach. Compared with a batch method, the MEKF gives more accurate results in the dynamic motion estimation problem.

This paper is organized as follows. Section 21.2 reviews the basic knowledge of Kalman filter techniques. Section 21.3 represents the 3-D line motion model in geometric algebra  $\mathcal{G}_{3,0,1}^+$  and gives an outline of the geometric algebra of rotors and motors. In section 21.4 we present the motor extended Kalman filter algorithm. Section 21.5 provides the experimental results of our MEKF, and finally, the conclusions are presented in section 21.6.

## 21.2 Kalman Filter Techniques

We will review in this section the principal equations for both the Kalman filter and the extended Kalman filter [126], [170] in order to introduce the necessary notations for the following sections.

### 21.2.1 The Kalman Filter

Consider a dynamical system whose state is described by a linear, vector difference equation. The system dynamic model is given by

$$\mathbf{X}_i = \Phi_{i/i-1} \mathbf{X}_{i-1} + \mathbf{W}_i. \quad (21.4)$$

The state of the system at  $t_i$  is given by the  $n$ -dimensional vector  $\mathbf{X}_i$ .  $\Phi_{i/i-1}$  is an  $n \times n$  matrix and  $\mathbf{W}_i$  is a vector random sequence with known statistics

$$E[\mathbf{W}_i] = \mathbf{0}, \quad i = 0, 1, \dots \quad (21.5)$$

$$E[\mathbf{W}_i \mathbf{W}_j^T] = \mathbf{Q}_i \delta_{ij} \quad (21.6)$$

where  $\delta_{ij}$  is the Kronecker delta function. The matrix  $\mathbf{Q}_i$  is assumed to be nonnegative-definite.

Suppose that at each time  $t_i$  there is available an  $m$ -dimensional vector of measurement  $\mathbf{Z}_i$  that is linearly related to the state and which is corrupted by additive noise  $\mathbf{V}_i$ .

$$\mathbf{Z}_i = \mathcal{H}_i \mathbf{X}_i + \mathbf{V}_i \quad (21.7)$$

$\mathcal{H}_i$  is a known  $m \times n$  observation matrix. The vector  $\mathbf{V}_i$  is an additive, random sequence with known statistics

$$E[\mathbf{V}_i] = \mathbf{0}, \quad i = 0, 1, \dots \quad (21.8)$$

$$E[\mathbf{V}_i \mathbf{V}_j^T] = \mathbf{C}_i \delta_{ij}. \quad (21.9)$$

The matrix  $\mathbf{C}_i$  is assumed to be nonnegative-definite.

Further, assume that the random processes  $\mathbf{W}_i$  and  $\mathbf{V}_i$  are mutually uncorrelated. These processes will also be called white noise sequence. That means

$$E[\mathbf{W}_i \mathbf{V}_j^T] = \mathbf{O} \quad i = 0, 1, \dots \quad (21.10)$$

matrix  $\mathbf{O}$  is null matrix.

Given the preceding models ((21.4) and (21.7)), we shall determine an estimate  $\hat{\mathbf{X}}_i$  of the state at  $t_i$  that is a linear combination of an estimate  $\hat{\mathbf{X}}_{i-1}$  at  $t_{i-1}$  and the measurement data  $\mathbf{Z}_i$  at  $t_i$ . By defining an unknown gain matrix  $\mathcal{K}_i$  ( $n \times m$ ), the estimate  $\hat{\mathbf{X}}_i$  is given by

$$\hat{\mathbf{X}}_i = \Phi_{i/i-1} \hat{\mathbf{X}}_{i-1} + \mathcal{K}_i [\mathbf{Z}_i - \mathcal{H}_i \Phi_{i/i-1} \hat{\mathbf{X}}_{i-1}] \quad (21.11)$$

The matrix  $\mathcal{K}_i$  shall be determined so that the estimate must be “best” in the sense that the expected value of the sum of the squares of the error in the estimate is a minimum. That is, the  $\hat{\mathbf{X}}_i$  is to be chosen so that

$$E_{min} = \text{Min}\{E[(\hat{\mathbf{X}}_i - \mathbf{X}_i)^T (\hat{\mathbf{X}}_i - \mathbf{X}_i)]\}. \quad (21.12)$$

Equation (21.12) is equivalent to minimization of the trace of state error covariance matrix  $\mathcal{P}_i$

$$E_{min} = \text{Min}\{\text{trace} \mathcal{P}_i\} = \text{Min}\{\text{trace} E[(\hat{\mathbf{X}}_i - \mathbf{X}_i)(\hat{\mathbf{X}}_i - \mathbf{X}_i)^T]\}. \quad (21.13)$$

By substituting (21.7) into (21.11), and then substituting (21.11) and (21.4) into (21.13), we can see that the trace of matrix  $\mathcal{P}_i$  will be minimized by choosing the optimal gain matrix  $\mathcal{K}_i$  such as

$$\mathcal{K}_i = \mathcal{P}_{i/i-1} \mathcal{H}_i^T (\mathcal{H}_i \mathcal{P}_{i/i-1} \mathcal{H}_i^T + \mathbf{C}_i)^{-1}, \quad (21.14)$$

where  $\mathcal{P}_{i/i-1}$  is called predicted state error covariance matrix

$$\mathcal{P}_{i/i-1} = \Phi_{i/i-1} \mathcal{P}_i \Phi_{i/i-1}^T + \mathcal{Q}_i, \quad (21.15)$$

which is the error covariance matrix of the predicted state  $\hat{\mathbf{X}}_{i/i-1}$

$$\hat{\mathbf{X}}_{i/i-1} = \Phi_{i/i-1} \hat{\mathbf{X}}_i. \quad (21.16)$$

With this optimal gain matrix  $\mathcal{K}_i$ , the matrix  $\mathcal{P}_i$  reduces to

$$\mathcal{P}_i = \mathcal{P}_{i/i-1} - \mathcal{K}_i \mathcal{H}_i \mathcal{P}_{i/i-1}. \quad (21.17)$$

Equations (21.11), (21.15), (21.14) and (21.17) constitute the Kalman filter for the model of the system (21.4) and that of the measurement (21.7), respectively.

Looking at (21.14), we see that as the measurement error covariance matrix  $\mathbf{C}_i$  approaches zero, the gain matrix  $\mathbf{K}_i$  weights the residual more heavily. Specifically,

$$\lim_{\mathbf{C}_i \rightarrow \mathbf{O}} \mathbf{K}_i = \mathbf{H}_i^{-1}. \quad (21.18)$$

On the other hand, as the estimated state error covariance  $\mathbf{P}_i$  approaches zero, the gain  $\mathbf{K}_i$  weights the residual less heavily. Specifically,

$$\lim_{\mathbf{P}_i \rightarrow \mathbf{O}} \mathbf{K}_i = \mathbf{O}. \quad (21.19)$$

Another way of thinking about the weighting by  $\mathbf{K}_i$  is that as the measurement error covariance matrix  $\mathbf{C}_i$  approaches zero, the actual measurement  $\mathbf{Z}_i$  is "trusted" more and more, while the predicted state  $\Phi_{i/i-1} \hat{\mathbf{X}}_i$  is trusted less and less. On the other hand, as the estimated state error covariance  $\mathbf{P}_i$  approaches zero the actual measurement  $\mathbf{Z}_i$  is trusted less and less, while the predicted state  $\Phi_{i/i-1} \hat{\mathbf{X}}_i$  (the dynamic model) is trusted more and more.

### 21.2.2 The Extended Kalman Filter

As described in section 21.2.1, the Kalman filter addresses the general problem of trying to estimate the state  $\mathbf{X}_i$  of a discrete-time controlled process that is governed by a linear stochastic difference equation. But what happens if the process and (or) the relation between the measurement and the state is non-linear? Some of the most interesting and successful applications of Kalman filtering are concerned with such situations. A Kalman filter that linearizes about the current predicted state  $\hat{\mathbf{X}}_{i/i-1}$  and measurement  $\mathbf{Z}_i$  is referred to as an extended Kalman filter or EKF.

In computer vision the measurement model is usually found to be described by a nonlinear observation equation  $\mathbf{f}_i(\mathbf{Z}_{0,i}, \mathbf{X}_i) = \mathbf{0}$ . The parameter  $\mathbf{Z}_{0,i}$  is the accurate measurement. In practice, such measurement is affected by random errors. We assume that the measurement system is disturbed by additive white noise, i.e., the real observed measurement  $\mathbf{Z}_i$  is expressed as

$$\mathbf{Z}_i = \mathbf{Z}_{0,i} + \mathbf{V}_i, \quad (21.20)$$

the statistics of noise  $\mathbf{V}_i$  are given by (21.8) and (21.9).

For applying the Kalman filter technique, we must expand the nonlinear observation equation into a first order Taylor series about  $(\mathbf{Z}_i, \hat{\mathbf{X}}_{i/i-1})$

$$\begin{aligned} \mathbf{f}_i(\mathbf{Z}_{0,i}, \mathbf{X}_i) &= \mathbf{f}_i(\mathbf{Z}_i, \hat{\mathbf{X}}_{i/i-1}) + \\ &+ \frac{\partial \mathbf{f}_i(\mathbf{Z}_i, \hat{\mathbf{X}}_{i/i-1})}{\partial \mathbf{Z}_{0,i}} (\mathbf{Z}_{0,i} - \mathbf{Z}_i) + \\ &+ \frac{\partial \mathbf{f}_i(\mathbf{Z}_i, \hat{\mathbf{X}}_{i/i-1})}{\partial \mathbf{X}_i} (\mathbf{X}_i - \hat{\mathbf{X}}_{i/i-1}) + \mathbf{R}_2 = \mathbf{0}. \end{aligned} \quad (21.21)$$

By ignoring the second order term  $\mathbf{R}_2$ , the linearized measurement equation (21.21) becomes

$$\mathbf{Y}_i = \mathcal{H}_i \mathbf{X}_i + \mathbf{N}_i, \quad (21.22)$$

where  $\mathbf{Y}_i$  is the new measurement vector,  $\mathbf{N}_i$  is the noise vector of the new measurement, and  $\mathcal{H}_i$  is the linearized transformation matrix. The components of the equation (21.22) are given by

$$\mathbf{Y}_i = -\mathbf{f}_i(\mathbf{Z}_i, \hat{\mathbf{X}}_{i/i-1}) + \frac{\partial \mathbf{f}_i(\mathbf{Z}_i, \hat{\mathbf{X}}_{i/i-1})}{\partial \mathbf{X}_i} \hat{\mathbf{X}}_{i/i-1},$$

$$\mathcal{H}_i = \frac{\partial \mathbf{f}_i(\mathbf{Z}_i, \hat{\mathbf{X}}_{i/i-1})}{\partial \mathbf{X}_i},$$

$$\mathbf{N}_i = \frac{\partial \mathbf{f}_i(\mathbf{Z}_i, \hat{\mathbf{X}}_{i/i-1})}{\partial \mathbf{Z}_{0,i}} (\mathbf{Z}_{0,i} - \mathbf{Z}_i),$$

$$E[\mathbf{N}_i] = \mathbf{0},$$

$$E[\mathbf{N}_i \mathbf{N}_i^T] = \mathbf{C}_{i/i-1}$$

$$= \frac{\partial \mathbf{f}_i(\mathbf{Z}_i, \hat{\mathbf{X}}_{i/i-1})}{\partial \mathbf{Z}_{0,i}} \mathbf{C}_i \frac{\partial \mathbf{f}_i(\mathbf{Z}_i, \hat{\mathbf{X}}_{i/i-1})^T}{\partial \mathbf{Z}_{0,i}},$$

where  $\mathbf{C}_i$  is given by the statistics of measurement (21.9). This linearized equation (21.22) is a general form for a nonlinear model. We will use this form for our particular nonlinear measurement model later in section 21.4.

### 21.3 3-D Line Motion Model

A line is one of the basic rigid geometric entities. In Euclidean space  $E_3$ , the operation of the line rigid motion is nonlinear. Whereas using the 4-D geometric algebra  $\mathcal{G}_{3,0,1}^+$ , also called motor algebra, the transformation becomes linear. In this section we first introduce the structure of the geometric algebra  $\mathcal{G}_{3,0,1}^+$ , and then give the Plücker line model and its motion model in  $\mathcal{G}_{3,0,1}^+$ .

#### 21.3.1 Geometric Algebra $\mathcal{G}_{3,0,1}^+$ and Plücker Line Model

Given a homogeneous extension of the Euclidean space  $E_3$  by an orthonormal set of vectors  $\gamma_1, \gamma_2, \gamma_3, \gamma_4$ , which in geometric algebra  $\mathcal{G}_{3,0,1}^+$  satisfy:

$$\gamma_i^2 = 1 \quad \text{for } i = 1, 2, 3, \quad (21.23)$$

$$\gamma_4^2 = 0, \quad (21.24)$$

$$\gamma_i \gamma_j = -\gamma_j \gamma_i \quad \text{for } i \neq j. \quad (21.25)$$

The basis of the linear space spanned by  $\mathcal{G}_{3,0,1}^+$  is composed by one scalar, six bivectors, and one pseudoscalar, that means the basis  $\mathcal{B}_{\mathcal{G}_{3,0,1}^+}$  is

$$\mathcal{B}_{\mathcal{G}_{3,0,1}^+} = \{1, \gamma_2\gamma_3, \gamma_3\gamma_1, \gamma_1\gamma_2, \gamma_4\gamma_1, \gamma_4\gamma_2, \gamma_4\gamma_3, I = \gamma_1\gamma_2\gamma_3\gamma_4\}, \quad (21.26)$$

with  $I^2 = 0$ .

A multivector  $\mathbf{A} \in \mathcal{G}_{3,0,1}^+$ ,

$$\begin{aligned} \mathbf{A} = & a_0 + a_1\gamma_2\gamma_3 + a_2\gamma_3\gamma_1 + a_3\gamma_1\gamma_2 + \\ & + I(a'_0 + a'_1\gamma_2\gamma_3 + a'_2\gamma_3\gamma_1 + a'_3\gamma_1\gamma_2), \end{aligned} \quad (21.27)$$

can be also expressed in a condensed dual form

$$\mathbf{A} = \mathbf{B} + I\mathbf{B}', \quad (21.28)$$

where  $\mathbf{B}$  and  $\mathbf{B}'$  are equivalent to quaternions.

A line  $\mathbf{L}$  with Plücker coordinates in  $\mathcal{G}_{3,0,1}^+$  can be represented as

$$\mathbf{L} = \mathbf{n} + I\mathbf{m}, \quad (21.29)$$

where  $\mathbf{n}$  and  $\mathbf{m}$  are bivectors,

$$\mathbf{n} = n_1\gamma_2\gamma_3 + n_2\gamma_3\gamma_1 + n_3\gamma_1\gamma_2 \quad (21.30)$$

$$\mathbf{m} = m_1\gamma_2\gamma_3 + m_2\gamma_3\gamma_1 + m_3\gamma_1\gamma_2. \quad (21.31)$$

Here  $\mathbf{n}$  is the direction of the line and  $\mathbf{m}$  is its moment. Any point  $\mathbf{p}$  on the line,

$$\mathbf{p} = p_1\gamma_2\gamma_3 + p_2\gamma_3\gamma_1 + p_3\gamma_1\gamma_2, \quad (21.32)$$

satisfies

$$\mathbf{m} = \mathbf{p} \wedge \mathbf{n}. \quad (21.33)$$

If  $\mathbf{n}$  is the normal direction of the line, then the norm of the moment calculated by (21.33) is the distance from the origin to the line (see Fig. 21.2).

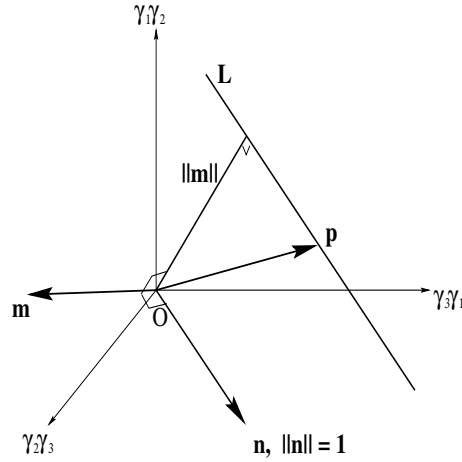


Fig. 21.2. Plücker coordinates of a line  $\mathbf{L}$

### 21.3.2 Plücker Line Motion Model in $\mathcal{G}_{3,0,1}^+$

In general, rigid motion consists of rotation and translation. The rotation is defined by both its rotation axis and rotation angle. A certain rigid motion has a unique rotation angle and a unique rotation axis direction, but the rotation axis can be placed anywhere in a 3-D coordinate system, the corresponding translation is then dependent on the position of the rotation axis. There are two positions of rotation axis having particular meaning. One is the axis passing through the origin of a reference coordinate system, the translation is applied after rotation. The other is so called screw motion, the rotation axis is in such a place that a rigid motion consists of rotation about this axis in space through an angle of  $\theta$ , followed by translation along the same axis by an amount  $d$ . The screw motion plays a very important role in rigid motion study [178]. In this section, we will discuss the features of motion of lines in Plücker coordinates.

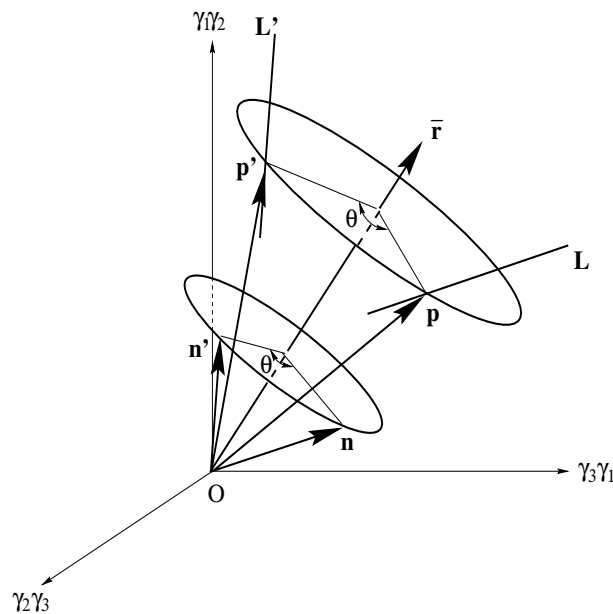


Fig. 21.3. The representation of pure rotation of a line

We first discuss the case of pure rotation as depicted in Fig. 21.3. The line is rotated by an angle  $\theta$  about an axis  $\bar{r}$  going through the origin  $O$ ,  $\bar{r}$  is a unit bivector. We can use a unit rotor  $\mathbf{R}$  to represent this rotation,

$$\begin{aligned}
\mathbf{R} &= r_0 + r_1\gamma_2\gamma_3 + r_2\gamma_3\gamma_1 + r_3\gamma_1\gamma_2 \\
&= r_0 + \mathbf{r} \\
&= \cos(\theta/2) + \sin(\theta/2)\bar{\mathbf{r}}
\end{aligned} \tag{21.34}$$

$$\tilde{\mathbf{R}} = r_0 - r_1\gamma_2\gamma_3 - r_2\gamma_3\gamma_1 - r_3\gamma_1\gamma_2 = r_0 - \mathbf{r}, \tag{21.35}$$

where  $\tilde{\mathbf{R}}$  is the inversion of  $\mathbf{R}$  with the constraint

$$\mathbf{R}\tilde{\mathbf{R}} = r_0^2 - \mathbf{r} \cdot \mathbf{r} = 1. \tag{21.36}$$

$\mathbf{L} = \mathbf{n} + I\mathbf{m}$  and  $\mathbf{L}' = \mathbf{n}' + I\mathbf{m}'$  are line coordinates before and after motion.  $\mathbf{p}$  is a point on the line  $\mathbf{L}$ , after motion it goes to  $\mathbf{p}'$ . Then

$$\begin{aligned}
\mathbf{L}' &= \mathbf{n}' + I\mathbf{m}' \\
&= \mathbf{R}\mathbf{n}\tilde{\mathbf{R}} + I(\mathbf{R}\mathbf{p}\tilde{\mathbf{R}}) \wedge (\mathbf{R}\mathbf{n}\tilde{\mathbf{R}}) \\
&= \mathbf{R}\mathbf{n}\tilde{\mathbf{R}} + I\mathbf{R}(\mathbf{p} \wedge \mathbf{n})\tilde{\mathbf{R}} \\
&= \mathbf{R}(\mathbf{n} + I\mathbf{m})\tilde{\mathbf{R}} \\
&= \mathbf{R}\mathbf{L}\tilde{\mathbf{R}},
\end{aligned} \tag{21.37}$$

In the case of pure translation  $\mathbf{t}$ , where  $\mathbf{t}$  is the bivector,

$$\mathbf{t} = t_1\gamma_2\gamma_3 + t_2\gamma_3\gamma_1 + t_3\gamma_1\gamma_2,$$

the direction  $\mathbf{n}$  of the line  $\mathbf{L}$  remains unchanged. A point  $\mathbf{p}$  on the line is moving to  $\mathbf{p}' = \mathbf{p} + \mathbf{t}$ . The translated line  $\mathbf{L}'$  is given by

$$\begin{aligned}
\mathbf{L}' &= \mathbf{n}' + I\mathbf{m}' \\
&= \mathbf{n} + I(\mathbf{p} + \mathbf{t}) \wedge \mathbf{n} \\
&= \mathbf{n} + I(\mathbf{m} + \mathbf{t} \wedge \mathbf{n}) \\
&= \mathbf{n} + I(\mathbf{m} + (\mathbf{t}\mathbf{n} - \mathbf{n}\mathbf{t})/2) \\
&= (1 + I\frac{\mathbf{t}}{2})(\mathbf{n} + I\mathbf{m})(1 - I\frac{\mathbf{t}}{2}) \\
&= \mathbf{T}\mathbf{L}\tilde{\mathbf{T}}
\end{aligned} \tag{21.38}$$

With line rotation model (21.37) and translation model (21.38), the transformation of a line (see Fig. 21.4) can be modeled by, e.g., applying a rotation  $\mathbf{R}$  followed by a translation  $\mathbf{T}$

$$\begin{aligned}
\mathbf{L}' &= \mathbf{T}\mathbf{R}\mathbf{L}\tilde{\mathbf{R}}\tilde{\mathbf{T}} \\
&= \mathbf{M}\mathbf{L}\tilde{\mathbf{M}},
\end{aligned} \tag{21.39}$$

where  $\mathbf{M}$  is a motor ,

$$\mathbf{M} = \mathbf{T}\mathbf{R} = (1 + I\frac{\mathbf{t}}{2})\mathbf{R} = \mathbf{R} + I\mathbf{R}' = r_0 + \mathbf{r} + I(r'_0 + \mathbf{r}') \tag{21.40}$$

$$\tilde{\mathbf{M}} = \tilde{\mathbf{R}}\tilde{\mathbf{T}} = \tilde{\mathbf{R}}(1 - I\frac{\mathbf{t}}{2}) = \tilde{\mathbf{R}} + I\tilde{\mathbf{R}}' \tag{21.41}$$

and

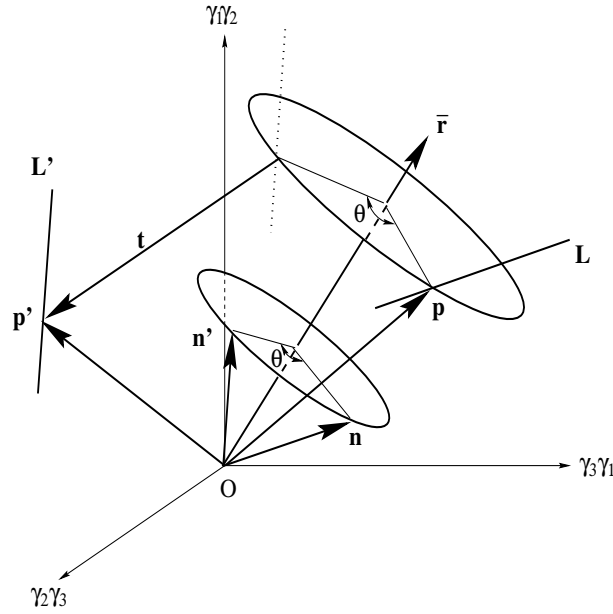


Fig. 21.4. The representation of rigid motion of a line

$$\begin{aligned}
 M\tilde{M} &= (1 + I\frac{\mathbf{t}}{2})\mathbf{R}\tilde{\mathbf{R}}(1 - I\frac{\mathbf{t}}{2}) = 1 \\
 &= (\mathbf{R} + I\mathbf{R}')(\tilde{\mathbf{R}} + I\tilde{\mathbf{R}}') = 1 + I(\mathbf{R}\tilde{\mathbf{R}}' + \mathbf{R}'\tilde{\mathbf{R}}).
 \end{aligned} \tag{21.42}$$

Deduced from the dual part of (21.42) we then get the following constraint

$$\mathbf{R}\tilde{\mathbf{R}}' + \mathbf{R}'\tilde{\mathbf{R}} = 2(r_0r'_0 - \mathbf{r} \cdot \mathbf{r}') = 0. \tag{21.43}$$

As we mentioned above, the motion can also be seen as a screw motion.

First let us consider a line  $\mathbf{L}$  rotating about another straight line  $\mathbf{L}_s = \bar{\mathbf{r}} + I\mathbf{t}_c \wedge \bar{\mathbf{r}}$  by an angle  $\theta$ , where the rotation axis  $\mathbf{L}_s$  is in some general position of a 3-D coordinate system and  $\mathbf{t}_c$  is pointing to an arbitrary point on  $\mathbf{L}_s$ . We call such a rotation as general rotation  $\mathbf{R}_s$ .  $\mathbf{R}_s$  can be seen as a combined motion, represented by a translation  $-\mathbf{t}_c$  first, then a rotation by rotor  $\mathbf{R}$ , finally followed by translation  $\mathbf{t}_c$ . That means, we first translate the rotation axis  $\mathbf{L}_s$  to pass the origin of the 3-D coordinate system, after that we perform a rotation and finally we translate this axis  $\mathbf{L}_s$  back to its original position:

$$\begin{aligned}
 \mathbf{R}_s &= (1 + I\mathbf{t}_c/2)(\cos(\theta/2) + \sin(\theta/2)\bar{\mathbf{r}})(1 - I\mathbf{t}_c/2) \\
 &= \cos(\theta/2) + \sin(\theta/2)(\bar{\mathbf{r}} + I\mathbf{t}_c \wedge \bar{\mathbf{r}}) \\
 &= \cos(\theta/2) + \sin(\theta/2)\mathbf{L}_s.
 \end{aligned} \tag{21.44}$$

A line rotated in this way can be easily given by

$$\begin{aligned} \mathbf{L}' &= \mathbf{n}' + I\mathbf{m}' \\ &= \mathbf{R}_s \mathbf{L} \tilde{\mathbf{R}}_s. \end{aligned} \quad (21.45)$$

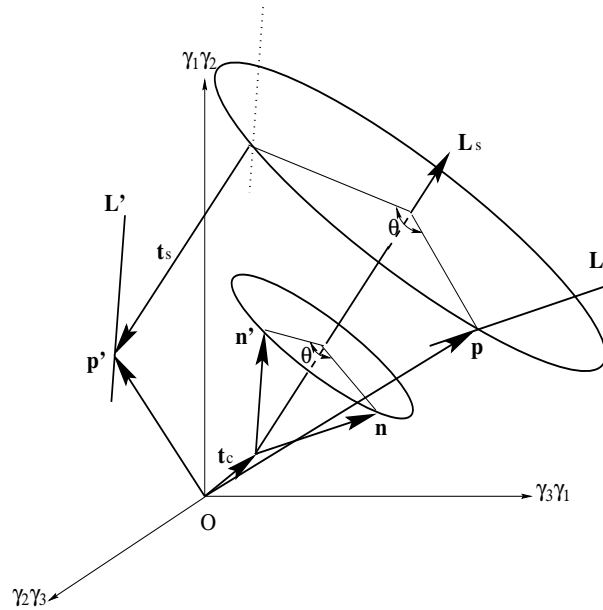


**Fig. 21.5.** The representation of screw motion of a line

Now, we can describe a screw motion easily. A screw motion is the combination of a general rotation, represented by  $\mathbf{R}_s$  and a translation  $\mathbf{t}_s$  which is parallel to the line  $\mathbf{L}_s$ , see Fig. 21.5. The screw motion equation is

$$\begin{aligned} \mathbf{L}' &= \mathbf{T}_s \mathbf{R}_s \mathbf{L} \tilde{\mathbf{R}}_s \tilde{\mathbf{T}}_s \\ &= \mathbf{M} \mathbf{L} \tilde{\mathbf{M}}. \end{aligned} \quad (21.46)$$

From the above discussion we see that using motor algebra, we can deal with rigid motion easily and efficiently. For example, if we use matrix algebra to describe a rigid motion, we must deal with 12 parameters, 9 for rotation and 3 for translation, using 6 constraints. In motor algebra, on the other hand, we only deal with 8 parameters and 2 constraints given by equations (21.36) and (21.43), respectively. Furthermore, motor algebra is algebraically isomorphic to dual-quaternion algebra. In reference [87], J. Funda et al. compared several methods of line-oriented representations of general spatial displacements of rigid bodies and drew the conclusion that dual-quaternion algebra is the best for the line transformations. As pointed out by D. Hestenes et al. in chapter 1, “the drawback of quaternions is that they are limited to 3-D applications, and even there they fail to make the important distinction

between vectors and bivectors”. “It should be clear that geometric algebra retains all of the advantages and none of the drawbacks of quaternions, while extending the range of applications enormously”. Another important advantage is that motors and rotors are both spinors. In spinor representation of Euclidean transformation, the group of several transformations corresponds to the geometric product of the spinors representing these transformations. We will use (21.46) for the motion estimation which will be discussed in the following section.

### 21.3.3 Interpretation of the Plücker Line Motion Model in Linear Algebra

The Plücker line motion model presented in the last section is considered in geometric algebra  $\mathcal{G}_{3,0,1}^+$ . Because the EKF algorithm is computed in linear algebra, we should interpret the line motion model  $\mathbf{L}' = \mathbf{M}\mathbf{L}\tilde{\mathbf{M}}$  in the frame of linear algebra. This can be done by remembering that  $\mathcal{G}_{3,0,1}^+$  spans the 8-dimensional linear space represented by (21.26), which is the union of a real and a dual 4-dimensional subspace, respectively. In that space the lines are the basic geometric entities and their mutual relations correspond to linear transformations by rotors or motors. This is just as the rotation of points in  $E_3$  can be linearly transformed using a rotation matrix  $\mathcal{R}$ .

First let us see some basic conversions.

The multiplication of two rotors  $\mathbf{U}$  and  $\mathbf{V}$  in geometric algebra  $\mathcal{G}_{3,0,1}^+$  reads

$$\begin{aligned}\mathbf{W} &= \mathbf{U}\mathbf{V} = (u_0 + \mathbf{u})(v_0 + \mathbf{v}) \\ &= u_0v_0 + \mathbf{u} \cdot \mathbf{v} + u_0\mathbf{v} + v_0\mathbf{u} + \mathbf{u}\wedge\mathbf{v}.\end{aligned}\quad (21.47)$$

Multiplication of these two rotors in linear algebra is

$$\mathbf{W} = \mathbf{U}_{Rl}\mathbf{V} = \mathbf{V}_{Rr}\mathbf{U}, \quad (21.48)$$

where  $\mathbf{U} = (u_0 \ u_1 \ u_2 \ u_3)^T$ ,  $\mathbf{V} = (v_0 \ v_1 \ v_2 \ v_3)^T$  and

$$\mathbf{U}_{Rl} = \begin{pmatrix} u_0 & -u_1 & -u_2 & -u_3 \\ u_1 & u_0 & u_3 & -u_2 \\ u_2 & -u_3 & u_0 & u_1 \\ u_3 & u_2 & -u_1 & u_0 \end{pmatrix},$$

$$\mathbf{V}_{Rr} = \begin{pmatrix} v_0 & -v_1 & -v_2 & -v_3 \\ v_1 & v_0 & -v_3 & v_2 \\ v_2 & v_3 & v_0 & -v_1 \\ v_3 & -v_2 & v_1 & v_0 \end{pmatrix}.$$

We call  $\mathbf{U}_{Rl}$  “left-multiplication matrix of motor  $\mathbf{U}$ ” and  $\mathbf{V}_{Rr}$  “right-multiplication matrix of motor  $\mathbf{V}$ ”.

Multiplication of two motors  $\mathbf{S} = \mathbf{U} + I\mathbf{U}'$  and  $\mathbf{T} = \mathbf{V} + I\mathbf{V}'$  in geometric algebra  $\mathcal{G}_{3,0,1}^+$  results

$$\begin{aligned}\mathbf{Q} &= \mathbf{ST} = (\mathbf{U} + I\mathbf{U}')(\mathbf{V} + I\mathbf{V}') \\ &= \mathbf{UV} + I(\mathbf{UV}' + \mathbf{U}'\mathbf{V}).\end{aligned}\quad (21.49)$$

Here  $\mathbf{U}$ ,  $\mathbf{U}'$ ,  $\mathbf{V}$  and  $\mathbf{V}'$  are all in the form of rotors. Multiplication of these two motors in linear algebra is given by

$$\mathbf{Q} = \mathbf{S}_{Ml}\mathbf{T} = \mathcal{T}_{Mr}\mathbf{S},\quad (21.50)$$

where

$$\begin{aligned}\mathbf{S} &= (u_0 \ u_1 \ u_2 \ u_3 \ u'_0 \ u'_1 \ u'_2 \ u'_3)^T, \\ \mathbf{T} &= (v_0 \ v_1 \ v_2 \ v_3 \ v'_0 \ v'_1 \ v'_2 \ v'_3)^T, \\ \mathbf{S}_{Ml} &= \begin{pmatrix} \mathbf{U}_{Rl} & \mathbf{0}_{4 \times 4} \\ \mathbf{U}'_{Rl} & \mathbf{U}_{Rl} \end{pmatrix}, \\ \mathcal{T}_{Mr} &= \begin{pmatrix} \mathbf{V}_{Rr} & \mathbf{0}_{4 \times 4} \\ \mathbf{V}'_{Rr} & \mathbf{V}_{Rr} \end{pmatrix},\end{aligned}$$

We call  $\mathbf{S}_{Ml}$  “left-multiplication matrix of motor  $\mathbf{S}$ ” and  $\mathcal{T}_{Mr}$  “right-multiplication matrix of motor  $\mathbf{T}$ ”.

To convert the Plücker line motion model (21.46) to linear algebra we can handle the real and dual components  $\mathbf{n}$ ,  $\mathbf{m}$ ,  $\mathbf{n}'$  and  $\mathbf{m}'$  of the lines  $\mathbf{L}$  and  $\mathbf{L}'$  as rotors with zero scalar. By right multiplication of both sides of equation (21.46) by  $\mathbf{M}$  we get

$$\mathbf{L}'\mathbf{M} - \mathbf{M}\mathbf{L} = 0.\quad (21.51)$$

This results in the following linear motion equation

$$(\mathcal{L}'_{Ml} - \mathcal{L}_{Mr})\mathbf{M} = \mathcal{A}_M\mathbf{M} = \mathbf{0}.\quad (21.52)$$

The constraints of equations (21.36) and (21.43), respectively, now are

$$\mathbf{R}^T\mathbf{R} = 1,\quad (21.53)$$

$$\mathbf{R}^T\mathbf{R}' = 0,\quad (21.54)$$

with  $\mathbf{R} = (r_0 \ r_1 \ r_2 \ r_3)^T$ ,  $\mathbf{R}' = (r'_0 \ r'_1 \ r'_2 \ r'_3)^T$  and  $\mathbf{M} = \mathbf{R} + I\mathbf{R}'$ .

These properties will be used for the implementation of the MEKF algorithm in the next section.

## 21.4 The Motor Extended Kalman Filter

In this section, we will formulate the motor extended Kalman filter (MEKF) algorithm. For applying Kalman filter techniques which were introduced in section 21.2, we know that we must be given both a dynamic model and a measurement model. We will first present the dynamic model using motor as state, then linearize the measurement equation (21.52) to get a linearized measurement equation, use (21.53) and (21.54) to modify the estimation to construct a proper motor estimation and finally, we present the MEKF algorithm.

### 21.4.1 Discrete Dynamic Model Using Motor State

Let us assume that we have a rigid object moving in 3-D space with approximately known trajectory. The object includes a number of lines ( $\mathbf{L}^1, \mathbf{L}^2, \dots, \mathbf{L}^n, n \geq 2$ ), we use the notation  $\mathbf{L}$  to represent any one of these lines. The 3-D coordinates of these lines are sampled at a number of time instants  $t_0, t_1, \dots, t_N$ . Suppose at time  $t_i$ , the rigid motion parameters with respect to time  $t_0$  are described by the motor  $\mathbf{M}_i$ , the relationship of the Plücker coordinates of a line at time  $t_0$  (denoted as  $\mathbf{L}_0$ ) and at time  $t_i$  ( $\mathbf{L}_i$ ) in  $\mathcal{G}_{3,0,1}^+$  is

$$\mathbf{L}_i = \mathbf{M}_i \mathbf{L}_0 \tilde{\mathbf{M}}_i. \quad (21.55)$$

The change of motion parameters from time  $t_{i-1}$  to  $t_i$  is described by the motor  $\mathbf{V}_{i/i-1}$ , that is

$$\mathbf{L}_i = \mathbf{V}_{i/i-1} \mathbf{L}_{i-1} \tilde{\mathbf{V}}_{i/i-1}. \quad (21.56)$$

By substituting (21.55) into (21.56), we get

$$\begin{aligned} \mathbf{L}_i &= \mathbf{V}_{i/i-1} \mathbf{M}_{i-1} \mathbf{L}_0 \tilde{\mathbf{M}}_{i-1} \tilde{\mathbf{V}}_{i/i-1} \\ &= \mathbf{M}_i \mathbf{L}_0 \tilde{\mathbf{M}}_i. \end{aligned} \quad (21.57)$$

Then we get the ideal dynamic motion model

$$\mathbf{M}_i = \mathbf{V}_{i/i-1} \mathbf{M}_{i-1}. \quad (21.58)$$

The motor  $\mathbf{V}_{i/i-1}$  encodes the velocity information. For example, suppose the motion is a screw motion with rotation of constant angular velocity  $\omega$  about an axis of known line ( $\mathbf{L}_s = \bar{\mathbf{r}} + I\mathbf{t}_c \wedge \bar{\mathbf{r}}$ ) and with constant translation velocity  $\mathbf{v}_s$  which is parallel to the axis. The data are sampled by a constant time interval and such a time interval is normalized to 1, then

$$\mathbf{V}_{i/i-1} = \mathbf{V} = (1 + I\mathbf{v}_s/2)(\cos(\omega/2) + \sin(\omega/2)\mathbf{L}_s). \quad (21.59)$$

In real applications we can only know the relation between  $\mathbf{M}_{i-1}$  and  $\mathbf{M}_i$  approximately. That means that such a dynamic motion model has to contain a process noise  $\mathbf{W}_i$ . Thus, the real dynamic model is given by

$$\mathbf{M}_i = \mathbf{V}_{i/i-1} \mathbf{M}_{i-1} + \mathbf{W}_i, \quad (21.60)$$

where the statistics of  $\mathbf{W}_i$  is given by (21.5) and (21.6). In linear algebra, (21.60) is expressed as

$$\mathbf{M}_i = \mathbf{V}_{i/i-1, M} \mathbf{M}_{i-1} + \mathbf{W}_i. \quad (21.61)$$

It must be noted that the motion parameters  $\mathbf{M}$  and  $\mathbf{V}$  should be described in the same coordinate system of the line  $\mathbf{L}$ , which is spanned by the algebra  $\mathcal{G}_{3,0,1}^+$ .

#### 21.4.2 Linearization of the Measurement Model

It is obvious that in (21.52) the relation between the measurement  $\mathcal{A}_M$  and the state  $\mathbf{M}$  is nonlinear, we must therefore first linearize it.

Suppose the measurement  $\mathcal{A}_{M_i}$  is the true data  $\mathcal{A}_{M0,i}$  contaminated by measurement noise  $\mathcal{N}_{\mathcal{A}_{M,i}}$

$$\mathcal{A}_{M_i} = \mathcal{A}_{M0,i} + \mathcal{N}_{\mathcal{A}_{M,i}}. \quad (21.62)$$

The noise matrix  $\mathcal{N}_{\mathcal{A}_{M,i}}$  is zero mean and we know the covariance of every component of the noise matrix. We define a function  $\mathbf{f}_{M,i}$  depending on the variables  $(\mathcal{A}_{M0,i}, \mathbf{M}_i)$  as follows

$$\mathbf{f}_{M,i}(\mathcal{A}_{M0,i}, \mathbf{M}_i) = \mathcal{A}_{M0,i} \mathbf{M}_i = \mathbf{0}. \quad (21.63)$$

Expanding (21.63) into a first order Taylor series about the measurement and the predicted state  $(\mathcal{A}_{M_i}, \hat{\mathbf{M}}_{i/i-1})$ , we get

$$\begin{aligned} & \mathbf{f}_{M,i}(\mathcal{A}_{M0,i}, \mathbf{M}_i) \\ &= \mathbf{f}_{M,i}(\mathcal{A}_{M_i}, \hat{\mathbf{M}}_{i/i-1}) + \\ & \quad + \frac{\partial \mathbf{f}_{M,i}(\mathcal{A}_{M_i}, \hat{\mathbf{M}}_{i/i-1})}{\partial \mathbf{M}_i} (\mathbf{M}_i - \hat{\mathbf{M}}_{i/i-1}) + \\ & \quad + (\mathcal{A}_{M0,i} - \mathcal{A}_{M_i}) \frac{\partial \mathbf{f}_{M,i}(\mathcal{A}_{M_i}, \hat{\mathbf{M}}_{i/i-1})}{\partial \mathcal{A}_{M0,i}} + \mathbf{R}_2 \\ &= \mathbf{0}, \end{aligned} \quad (21.64)$$

where

$$\frac{\partial \mathbf{f}_{M,i}(\mathcal{A}_{M_i}, \hat{\mathbf{M}}_{i/i-1})}{\partial \mathbf{M}_i} = \mathcal{A}_{M_i}, \quad (21.65)$$

$$\frac{\partial \mathbf{f}_{M,i}(\mathcal{A}_{M_i}, \hat{\mathbf{M}}_{i/i-1})}{\partial \mathcal{A}_{M0,i}} = \hat{\mathbf{M}}_{i/i-1}. \quad (21.66)$$

Substituting (21.65) and (21.66) into (21.64), omitting the second order terms  $\mathbf{R}_2$ , and using (21.62), (21.64) can be written as follows

$$\begin{aligned}
& \mathcal{A}_{M_i} \hat{M}_{i/i-1} + \mathcal{A}_{M_i} (M_i - \hat{M}_{i/i-1}) + \\
& + (\mathcal{A}_{M_{0,i}} - \mathcal{A}_{M_i}) \hat{M}_{i/i-1} \\
= & \mathcal{A}_{M_i} \hat{M}_{i/i-1} + \mathcal{A}_{M_i} (M_i - \hat{M}_{i/i-1}) - \mathcal{N}_{\mathcal{A}_{M,i}} \hat{M}_{i/i-1} \\
= & \mathbf{0}.
\end{aligned} \tag{21.67}$$

Then the linearized measurement equation for MEKF at step  $i$  is

$$\begin{aligned}
Z_i &= -\mathcal{A}_{M_i} M_i + \mathcal{N}_{\mathcal{A}_{M,i}} \hat{M}_{i/i-1} \\
&= \mathcal{H}_i M_i + N_{Z,i} \\
&= \mathbf{0},
\end{aligned} \tag{21.68}$$

where  $\mathcal{H}_i = -\mathcal{A}_{M_i}$  and  $N_{Z,i} = \mathcal{N}_{\mathcal{A}_{M,i}} \hat{M}_{i/i-1}$ . The covariance matrix of  $N_{Z,i}$  is  $\mathcal{C}_i$ .

### 21.4.3 Constraints Problem

According to the Kalman filter algorithm ((21.11), (21.15), (21.14) and (21.17)), we can compute the estimation  $M_i^*$  as

$$\begin{aligned}
M_i^* &= \Phi_{i/i-1} \hat{M}_{i-1} + \mathcal{K}_i (Z_i - \mathcal{H}_i \Phi_{i/i-1} \hat{M}_{i-1}) \\
&= \mathcal{V}_{i/i-1, Ml} \hat{M}_{i-1} + \mathcal{K}_i (-\mathcal{H}_i \mathcal{V}_{i/i-1, Ml} \hat{M}_{i-1}) \\
&= (\mathbf{R}_i^{*T} \quad \mathbf{R}'_i^{*T})^T
\end{aligned} \tag{21.69}$$

The 4-dimensional vectors  $\mathbf{R}_i^*$  and  $\mathbf{R}'_i^*$  are the first 4 components and the last 4 components of  $M_i^*$ , respectively. They must be modified to satisfy the constraints (21.53) and (21.54). For the constraint (21.53), this can be done simply by

$$\hat{\mathbf{R}}_i = \frac{\mathbf{R}_i^*}{\|\mathbf{R}_i^*\|}. \tag{21.70}$$

But to satisfy the constraint (21.54) is not so simple. Now, we rewrite (21.54) as  $\mathbf{R}'^T \mathbf{R} = 0$ , this equation means that the rotor  $\mathbf{R}$  and the dual rotor  $\mathbf{R}'$ , in their vector form, must be orthogonal to each other. Unfortunately, the estimated rotor  $\mathbf{R}_i^*$  is usually not orthogonal to the estimated dual rotor  $\mathbf{R}'_i^*$ , see Figure 21.6. Suppose the angle between estimates  $\mathbf{R}_i^*$  and  $\mathbf{R}'_i^*$  is  $\varphi$ , then

$$\cos(\varphi) = \frac{\mathbf{R}'_i^{*T} \mathbf{R}_i^*}{\|\mathbf{R}'_i^*\| \cdot \|\mathbf{R}_i^*\|} \tag{21.71}$$

Using (21.70), (21.71) can be simplified by introducing the unit rotor  $\hat{\mathbf{R}}_i$  as

$$\cos(\varphi) = \frac{\mathbf{R}'_i^{*T} \hat{\mathbf{R}}_i}{\|\mathbf{R}'_i^*\|}. \tag{21.72}$$

It can be easily understood that the best modified dual rotor  $\hat{\mathbf{R}}'_i$  should be closest to the estimated dual rotor  $\mathbf{R}'_i^*$ . That means that the difference of

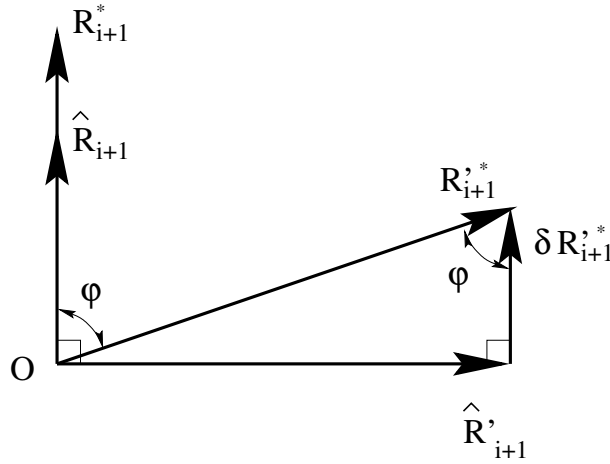


Fig. 21.6. Constraint of  $\hat{\mathbf{R}}^{*T} \hat{\mathbf{R}}'^* = 0$

these two vectors,  $\delta \mathbf{R}'_i^*$ , should be orthogonal to the modified dual rotor  $\hat{\mathbf{R}}'_i$  and should be parallel to the rotor  $\hat{\mathbf{R}}_i$ . In other words, the length of  $\delta \mathbf{R}'_i^*$  is  $\|\mathbf{R}'_i^*\| \cos(\varphi)$  and the direction of it is equal to that of the rotor  $\hat{\mathbf{R}}_i$ . Then,

$$\delta \mathbf{R}'_i^* = \|\mathbf{R}'_i^*\| \cos(\varphi) \hat{\mathbf{R}}_i = (\mathbf{R}'_i^{*T} \hat{\mathbf{R}}_i) \hat{\mathbf{R}}_i, \quad (21.73)$$

so that

$$\hat{\mathbf{R}}'_i = \mathbf{R}'_i^* - (\mathbf{R}'_i^{*T} \hat{\mathbf{R}}_i) \hat{\mathbf{R}}_i. \quad (21.74)$$

$\hat{\mathbf{R}}_i$  and  $\hat{\mathbf{R}}'_i$  are the modified estimations at  $i$  and satisfy the constraints (21.53) and (21.54).

#### 21.4.4 The MEKF Algorithm

The MEKF algorithm is summarized in Fig. 21.7. At time 0, it begins with a given initial predicted state  $\hat{M}_{1/0}$  and the initial predicted state error covariance matrix  $\mathcal{P}_{1/0}$  as a prediction of time 1. If we do not know the initial predicted state, we can simply set

$$\hat{M}_{1/0} = [1 \ 0 \ 0 \ 0 \ 0 \ 0 \ 0 \ 0]^T \quad (21.75)$$

$$\mathcal{P}_{1/0} = \mathbf{I}_{8 \times 8} \quad (21.76)$$

At time 1, we first compute the matrix  $\mathcal{H}_1$  of the linearized measurement equation and the Kalman gain matrix  $\mathcal{K}_1$ , then we can calculate the estimation  $M_1^*$ . This estimation must be modified to be  $\hat{M}_1$  which satisfies the motor constraints.  $\hat{M}_1$  serves as the result of the estimation and then we can get the prediction  $\hat{M}_{2/1}$  of time 2 by dynamic model. The MEKF will run recursively till time  $N$ . The MEKF algorithm is listed in Fig. 21.7.

It must be noted that the numerical instability of Kalman filter implementation is well known. Several techniques are developed to overcome those

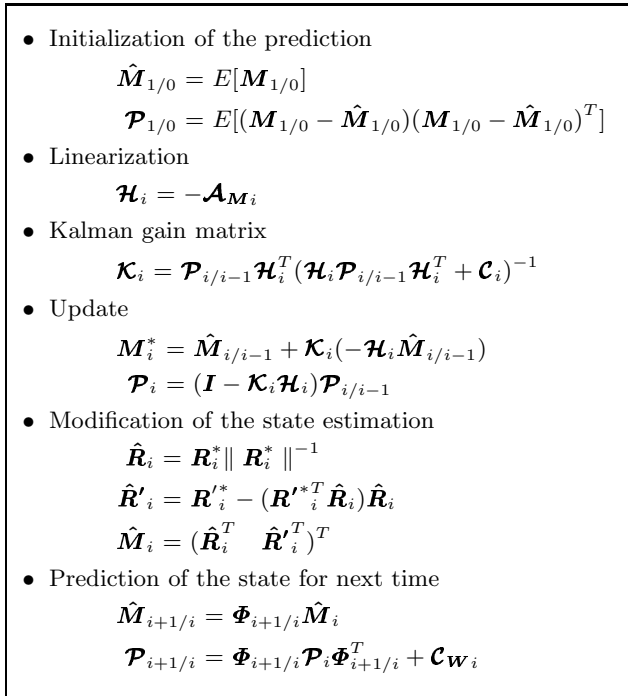


Fig. 21.7. MEKF algorithm

problems, such as square-root filtering and U-D factorization. See [170] for a thorough discussion.

#### 21.4.5 A Batch Method of Analytical Solution

In [247], Zhang and Faugeras have presented an analytical method to recover the motion parameters from Plücker line measurements. We will introduce it here for the purpose of comparing it with the method of the MEKF. This analytical solution can also be used for estimating the initial prediction in our MEKF algorithm.

Assume that there are  $n$  lines of the rigid object, which are measured before and after motion  $\mathbf{M}_i$ . The coordinates of these lines are  $\mathbf{L}_0^k = \mathbf{n}_0^k + \mathbf{I} \mathbf{m}_0^k$  and  $\mathbf{L}_i^k = \mathbf{n}_i^k + \mathbf{I} \mathbf{m}_i^k$ ,  $k = 1, 2, \dots, n$ , where the subscript numbers 0 and  $i$  correspond to the case before and after motion, respectively. The motor  $\mathbf{M}_i$  can also be seen as a combined motion of a rotation  $\mathbf{R}_i$  and a translation  $\mathbf{t}_i$ , which in  $\mathcal{G}_{3,0,1}^+$  satisfies

$$\mathbf{M}_i = (1 + \mathbf{I} \mathbf{t}_i / 2) \mathbf{R}_i. \quad (21.77)$$

Then, the relation between a line  $\mathbf{L}_0 = \mathbf{L}_0^k$  and the transformed line  $\mathbf{L}_i = \mathbf{L}_i^k$  is given by

$$\begin{aligned}
\mathbf{L}_i &= \mathbf{n}_i + I\mathbf{m}_i \\
&= \mathbf{M}_i \mathbf{L}_0 \tilde{\mathbf{M}}_i \\
&= (1 + I\mathbf{t}_i/2) \mathbf{R}_i (\mathbf{n}_0 + I\mathbf{m}_0) \tilde{\mathbf{R}}_i (1 - I\mathbf{t}_i/2) \\
&= \mathbf{R}_i \mathbf{n}_0 \tilde{\mathbf{R}}_i + I(\mathbf{R}_i \mathbf{m}_0 \tilde{\mathbf{R}}_i + (\mathbf{t}_i (\mathbf{R}_i \mathbf{n}_0 \tilde{\mathbf{R}}_i) - (\mathbf{R}_i \mathbf{n}_0 \tilde{\mathbf{R}}_i) \mathbf{t}_i)/2) \\
&= \mathbf{R}_i \mathbf{n}_0 \tilde{\mathbf{R}}_i + I(\mathbf{R}_i \mathbf{m}_0 \tilde{\mathbf{R}}_i + \mathbf{t}_i \wedge (\mathbf{R}_i \mathbf{n}_0 \tilde{\mathbf{R}}_i)). \tag{21.78}
\end{aligned}$$

By separating the real and dual part of above equation, we get

$$\mathbf{n}_i = \mathbf{R}_i \mathbf{n}_0 \tilde{\mathbf{R}}_i \tag{21.79}$$

$$\mathbf{m}_i = \mathbf{R}_i \mathbf{m}_0 \tilde{\mathbf{R}}_i + \mathbf{t}_i \wedge \mathbf{n}_i. \tag{21.80}$$

Because  $\mathbf{L}_0^k$  and  $\mathbf{L}_i^k$  are the noisy measurements, we use a least square method to estimate a best solution of rotation and translation. We determine first the rotation using (21.79) by minimizing the following criterion

$$E_{min} = Min\left\{\sum_{k=1}^n \|\mathbf{n}_i^k - \mathbf{R}_i \mathbf{n}_0^k \tilde{\mathbf{R}}_i\|^2\right\}. \tag{21.81}$$

After right-multiplying both sides of (21.79) with the rotor  $\mathbf{R}_i$ , we get

$$\mathbf{n}_i \mathbf{R}_i - \mathbf{R}_i \mathbf{n}_0 = \mathbf{0}. \tag{21.82}$$

In linear algebra, (21.82) is expressed as

$$(\mathbf{n}_i)_{Rl} \mathbf{R}_i - (\mathbf{n}_0)_{Rr} \mathbf{R}_i = \mathcal{A}_R \mathbf{R}_i = \mathbf{0}. \tag{21.83}$$

Then, (21.81) can be further restated as

$$E'_{min} = Min\left\{\sum_{k=1}^n \mathbf{R}_i^T \mathcal{A}_R^k T \mathcal{A}_R^k \mathbf{R}_i\right\} = Min\{\mathbf{R}_i^T \mathcal{A} \mathbf{R}_i\}, \tag{21.84}$$

where

$$\mathcal{A}_R^k = \sum_{k=1}^n ((\mathbf{n}_i^k)_{Rl} - (\mathbf{n}_0^k)_{Rr}), \tag{21.85}$$

$$\mathcal{A} = \sum_{k=1}^n \mathcal{A}_R^k T \mathcal{A}_R^k. \tag{21.86}$$

Since  $\mathcal{A}$  is a symmetric matrix and  $\|\mathbf{R}_i\| = 1$ , the solution to this problem is the 4-dimensional vector  $\tilde{\mathbf{R}}_i$  corresponding to the smallest eigenvalue of  $\mathcal{A}$ .

With the recovered rotation  $\tilde{\mathbf{R}}_i$  we can then determine the translation using (21.80). In linear algebra, (21.80) is expressed as

$$\mathbf{m}_i = \mathcal{R}_i \mathbf{m}_0 - (\mathbf{n}_i)_{\times} \mathbf{t}_i, \tag{21.87}$$

where

$$\mathcal{R}_i = (\mathbf{R}_i)_{Rl} (\tilde{\mathbf{R}}_i)_{Rr}, \tag{21.88}$$

and the matrix  $(\mathbf{n}_i)_\times$  is the skew-symmetric matrix of  $\mathbf{n}_i$ , which performs the outer product of the bivector  $\mathbf{n}_i$  with another bivector. If  $n_{1,i}$ ,  $n_{2,i}$  and  $n_{3,i}$  are three components of the bivector  $\mathbf{n}_i$ , then

$$(\mathbf{n}_i)_\times = \begin{pmatrix} 0 & n_{3,i} & -n_{2,i} \\ -n_{3,i} & 0 & n_{1,i} \\ n_{2,i} & -n_{1,i} & 0 \end{pmatrix}. \quad (21.89)$$

We estimate the translation  $\hat{\mathbf{t}}_i$  by minimizing the following criterion

$$E''_{min} = Min\left\{\sum_{k=1}^n \|\mathbf{m}_i^k - \hat{\mathcal{R}}_i \mathbf{m}_0^k + (\mathbf{n}_i^k)_\times \hat{\mathbf{t}}_i\|^2\right\}. \quad (21.90)$$

By differentiating the criterion (21.90) with respect to  $\mathbf{t}_0$  and setting the result equal to zero, we obtain

$$\sum_{k=1}^n 2 \left( \mathbf{m}_i^k - \hat{\mathcal{R}}_i \mathbf{m}_0^k + (\mathbf{n}_i^k)_\times \hat{\mathbf{t}}_i \right)^T (\mathbf{n}_i^k)_\times = \mathbf{0}. \quad (21.91)$$

Then,  $\hat{\mathbf{t}}_i$  can be solved by the equation:

$$\left( \sum_{k=1}^n (\mathbf{n}_i^k)_\times^T (\mathbf{n}_i^k)_\times \right) \hat{\mathbf{t}}_i = \sum_{k=1}^n (\mathbf{n}_i^k)_\times^T (\hat{\mathcal{R}}_i \mathbf{m}_0^k - \mathbf{m}_i^k). \quad (21.92)$$

It can be shown that the matrices  $\mathbf{A}$  and  $\mathbf{B} = \sum_{k=1}^n (\mathbf{n}_i^k)_\times (\mathbf{n}_i^k)_\times^T$  are always of full rank if two of the lines  $\mathbf{L}_i^k (k = 1..n)$  are non-parallel. In other words, to determine a unique motion displacement there must be at least two non-parallel lines.

## 21.5 Experimental Analysis of the MEKF

To further verify the analyses presented above and to demonstrate the performance of the MEKF algorithm, experiments using both simulated data and real 3-D reconstructed lines have been performed.

### 21.5.1 Simulation

The routine of the MEKF is programmed in MATLAB. The goal of the simulated experiments is to test the routine of MEKF, and by filter tuning to improve the accuracy and the converge rate of the estimate.

Let us suppose a rigid object is moving along a screw in 3-D with constant angular velocity  $\omega/2 = -\pi/15$  about an axis of known line ( $\mathbf{L}_s = \bar{\mathbf{r}} + I\mathbf{t}_c \wedge \bar{\mathbf{r}}$ ) and constant translation velocity  $\mathbf{v}_s = 0.3\bar{\mathbf{r}}$  which is parallel to the axis. A

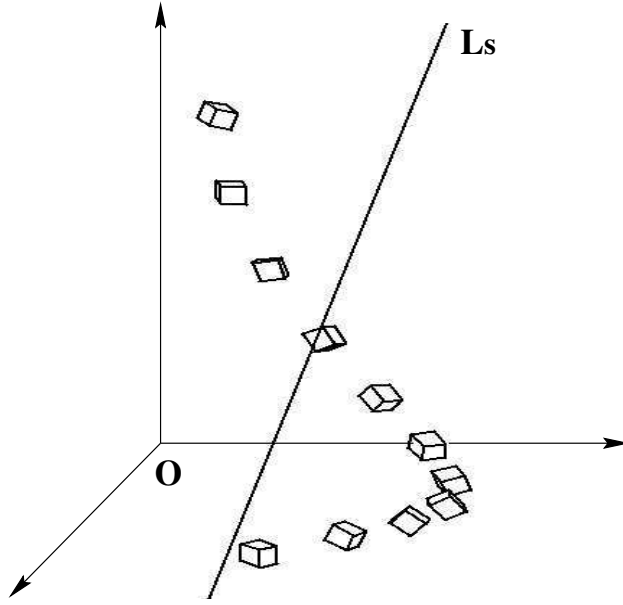


Fig. 21.8. The object moving in 3-D with screw trajectory

box moving in this way is shown in Fig. 21.8. The line  $\mathbf{L}_s$  is given by

$$\begin{aligned}\mathbf{L}_s &= \bar{\mathbf{r}} + I t_c \wedge \bar{\mathbf{r}} \\ &= 0.7071\gamma_2\gamma_3 + 0.3536\gamma_3\gamma_1 + 0.6124\gamma_1\gamma_2 + \\ &\quad + I(-0.7418\gamma_2\gamma_3 + 0.3813\gamma_3\gamma_1 + 0.6364\gamma_1\gamma_2).\end{aligned}$$

Assume the measurements are sampled by equal time intervals which are normalized to 1. Then the motion between times  $i-1$  and  $i$  can be described by the motor  $\mathbf{V}$ , which can be calculated by (21.59).

$$\begin{aligned}\mathbf{V} &= (1 + I\mathbf{v}_{s0}/2)(\cos(\omega/2) + \sin(\omega/2)\mathbf{L}_s) \\ &= (1 + I0.3\bar{\mathbf{r}}/2)(\cos(-\pi/15) + \sin(-\pi/15)\mathbf{L}_s) \\ &= 0.9832 - 0.1289\gamma_2\gamma_3 - 0.0645\gamma_3\gamma_1 - 0.1117\gamma_1\gamma_2 + \\ &\quad + I(-0.0266 + 0.2367\gamma_2\gamma_3 - 0.0188\gamma_3\gamma_1 - 0.0283\gamma_1\gamma_2).\end{aligned}\quad (21.93)$$

Then we get the dynamic motion equation in linear algebra

$$\mathbf{M}_i = \mathbf{V}_{Ml}\mathbf{M}_{i-1}.\quad (21.94)$$

In simulation, the real applied motion parameters  $\mathbf{V}_{i/i-1}$  between times  $i-1$  and  $i$  are contaminated by noise:

$$\begin{aligned}\omega_i &= \omega + n_{\omega_i}, \\ v_{s_i} &= v_s + n_{v_{s_i}}, \\ \mathbf{V}_{i/i-1} &= (1 + I\mathbf{v}_{s_i}/2)(\cos(\omega_i/2) + \sin(\omega_i/2)\mathbf{L}_s),\end{aligned}$$

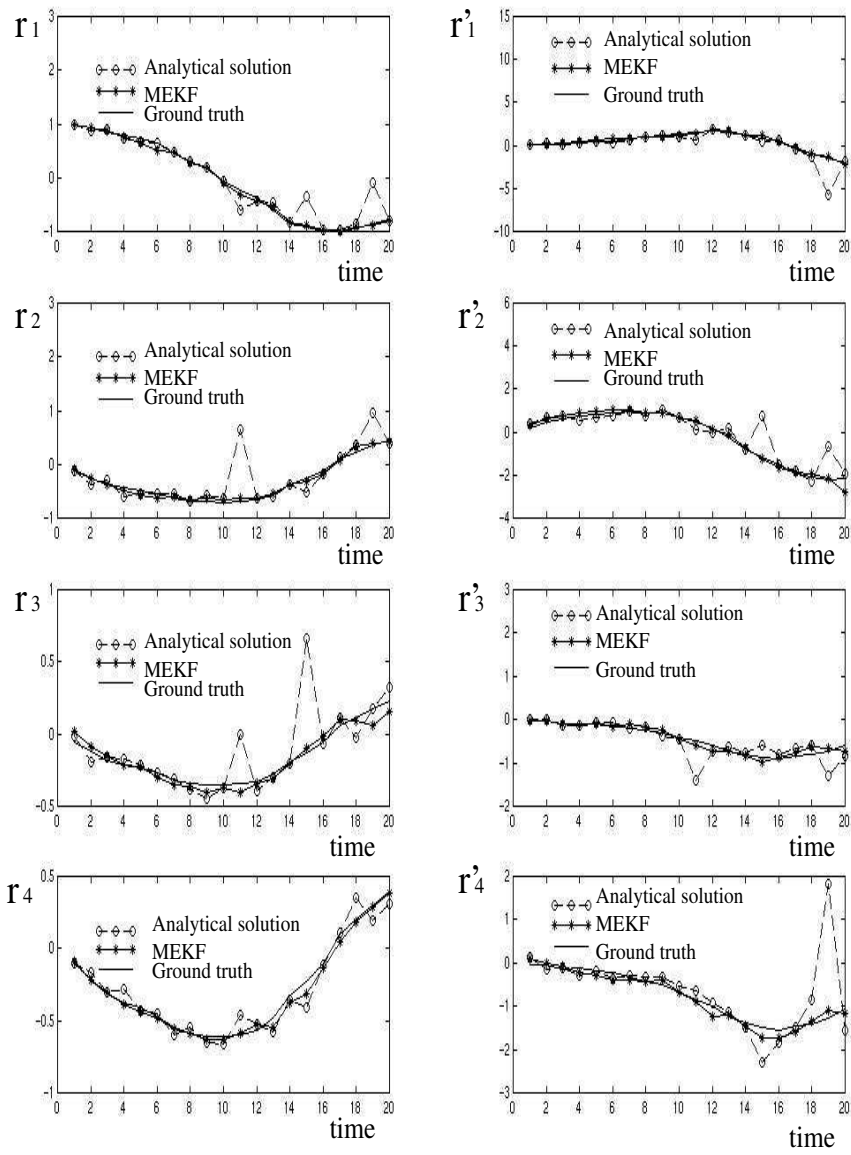


Fig. 21.9. The estimation results of the motor parameters by simulation

where the noises  $n_{\omega_i}$  and  $n_{v_{s_i}}$  are independent normally distributed with zero mean and known deviation  $\sigma_{\omega}$  and  $\sigma_{v_s}$ . Then the ground truth of motor trajectories  $\mathbf{M}_{0,i}$  can be computed by

$$\begin{aligned}\mathbf{M}_{0,i} &= \left( r_{0i} \ r_{1i} \ r_{2i} \ r_{3i} \ r'_{0i} \ r'_{1i} \ r'_{2i} \ r'_{3i} \right)^T \\ &= \mathcal{V}_{i/i-1}^{ML} \mathbf{M}_{0,i-1},\end{aligned}\quad (21.95)$$

with initial state  $\mathbf{M}_{0,0} = (1 \ 0 \ 0 \ 0 \ 0 \ 0 \ 0 \ 0)$ .

At  $i$ -th ( $i = 1, 2, \dots, N$ ) time step of MEKF algorithm we first generate two 3-D points  $\mathbf{x}'_0$  and  $\mathbf{y}'_0$  to define a line  $\mathbf{L}'_0$  in an observer coordinate frame A. The points are then moved to  $\mathbf{x}'_i$  and  $\mathbf{y}'_i$  by the motor  $\mathbf{M}_i = (\mathbf{V}_{i/i-1})^{ML} \mathbf{M}_{i-1}$  which can be decomposed to rotation  $\mathbf{R}_i$  and translation  $\mathbf{t}_i$ , where  $\mathbf{R}_i$  is the real part of  $\mathbf{M}_i$ . If  $\tilde{\mathbf{R}}_i$  is the dual part of  $\mathbf{M}_i$ , from (21.41) we can get  $\mathbf{t}_i = 2\mathbf{R}'_i \tilde{\mathbf{R}}_i$ .

The coordinate of this line after motion is  $\mathbf{L}'_i$  relative to the frame A. We obtain thus a pair of noise-free coordinates of the same line in two positions (the initial position  $\mathbf{L}'_0$  and the position  $\mathbf{L}'_i$  at time  $i$ ). To simulate the noisy observation, independent Gaussian noise with zero mean and known standard deviation  $\sigma$  is added to both lines  $\mathbf{L}'_0$  and  $\mathbf{L}'_{i+1}$  and we obtain thus the noisy observation  $\mathbf{L}_0$  and  $\mathbf{L}_i$ .

In Fig. 21.9, we show the eight components of motor trajectories estimated by MEKF algorithm and by batch method of the analytical solution. In MEKF algorithm we use the analytical solution to estimate the initial prediction. Comparing with ground truth, we can see that the MEKF gives more accurate and more stable estimates.

### 21.5.2 Real Experiment

Fig. 21.10 shows the physical setup of our experiment. Two grey-scale-CCD  $640 \times 480$  cameras are fastened to the last joint of the robot arm RX90. The RX90 has six rotation joints which can be controlled by six parameters (x, y, z, roll, pitch, and yaw). The coordinates (x, y, z) that describe the position of the end joint are referred to the base coordinate system  $W$  which is fixed on the base of the arm. The rotation parameters (roll, pitch, yaw) that describe the orientation of the end joint are Z-Y-Z Euler angles [50]. The sample object is placed below the cameras.

We want to estimate the relative motion between the end joint and the sample object based on the cameras' images while the arm is moving with a given trajectory.

In practice, we use 3 cameras to reconstruct a 3-D line. In the experimental setup, the third camera was realized by applying a certain motion to one of the cameras.

We have no ground truth of the relative motion of the sample object. But we can compare the estimation with the given motion trajectory of the robot arm. A coordinate system  $T$  which is fixed on the end joint is called a tool coordinate system. We control the robot arm by controlling the relative

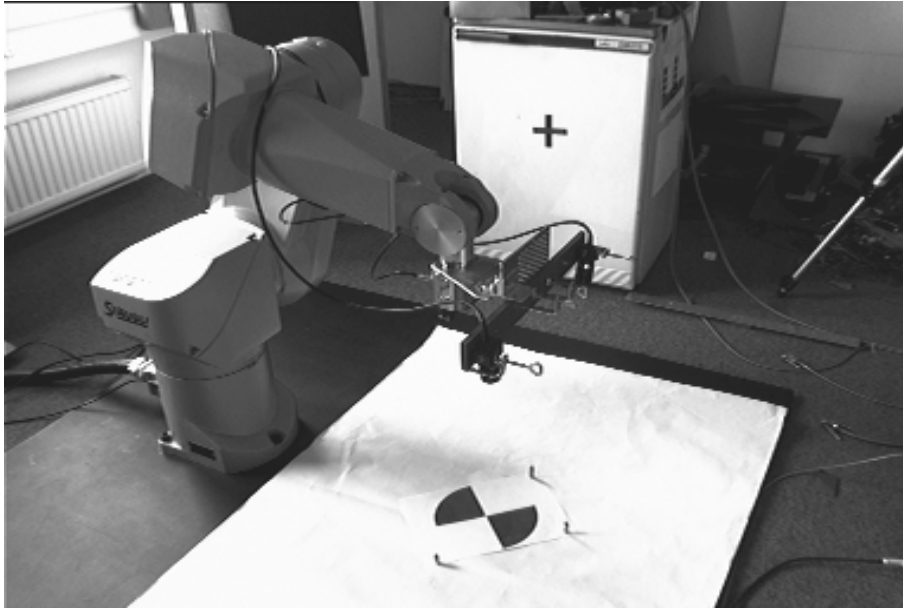


Fig. 21.10. The physical setup of the experiment

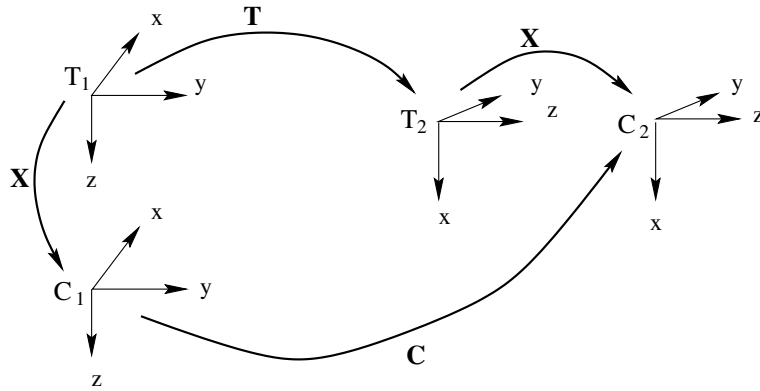


Fig. 21.11. The relationship between the tool system  $T$  and the camera system  $C$

position and orientation between the tool system  $T$  and the base system  $W$ . After camera calibration, we get a matrix  $\mathcal{P}$ , which describes the relationship between the point coordinates in the 2-D image and the correspondent 3-D world point coordinates with respect to a system  $C$  (up to a scalar  $\lambda$ ). The system  $C$  is fixed on the end joint and there exists a certain transformation  $\mathbf{X}$  between the tool system  $T$  and the system  $C$ , see Fig. 21.11. The transformation  $\mathbf{X}$  is determined by hand-eye calibration. If the tool system is transformed from  $T_1$  to  $T_2$  by transformation  $\mathbf{T}$ , the system  $C$  will be transformed from  $C_1$  to  $C_2$  by a certain transformation  $\mathbf{C}$ , which is given by

$$\mathbf{C} = \mathbf{X}\mathbf{T}\mathbf{X}^{-1}. \quad (21.96)$$

Using (21.96) we can compare the relative motion  $\mathbf{C}$  of the sample object referring to system  $C$  with the given motion  $\mathbf{T}$  of the robot arm.

The steps of the experiment are as follows:

- 1) Cameras calibration [77] to determine the  $\mathcal{P}$  matrix;
- 2) Hand-eye calibration [139] to determine the unknown transformation  $\mathbf{X}$ ; (an alternative would be [16] using motors)
- 3) Taking the images in discrete time steps with constant time intervals while the robot arm is moving, see Figs. 21.12 and 21.14;
- 4) Extracting 2-D lines from the images using Hough transformation [149] [186], see Figs. 21.13 and 21.15;
- 5) 3-D line reconstruction by 3 matched image lines [77], see Tab. 21.1 ;
- 6) Estimation the motion based on 3-D line observations using MEKF, see Fig. 21.16 .

The algorithm of motion estimation will run online recursively from step 3) to 6).

In our experiment, the given relative motion of the sample object with respect to system  $C$  is a screw motion with constant angular velocity  $\omega = -\pi/90$  and constant translation velocity  $\mathbf{v}_s = 0.2$  which is parallel to the rotation axis. The rotation axis  $\mathbf{L}_s$  is parallel to the z axis of the system  $C$ , and one point on  $\mathbf{L}_s$  is (1.5, 0, 0). In  $\mathcal{G}_{3,0,1}^+$  the screw axis  $\mathbf{L}_s$  is given by

$$\begin{aligned} \mathbf{L}_s &= \gamma_1\gamma_2 + I(1.5\gamma_2\gamma_3)\wedge(\gamma_1\gamma_2) \\ &= \gamma_1\gamma_2 + I1.5\gamma_3\gamma_1. \end{aligned} \quad (21.97)$$

Just like (21.93), the motor  $\mathbf{V}$  can be calculated as

$$\begin{aligned} \mathbf{V} &= (1 + I\mathbf{v}_{s0}/2)(\cos(\omega/2) + \sin(\omega/2)\mathbf{L}_s) \\ &= 0.9994 - 0.0349\gamma_1\gamma_2 + I(0.0035 - 0.0523\gamma_3\gamma_1 + 0.0999\gamma_1\gamma_2). \end{aligned} \quad (21.98)$$

The motor  $\mathbf{M}_{i+1}$  is in linear algebra given by

$$\mathbf{M}_i = \mathcal{V}_{MI}\mathbf{M}_{i-1}, \quad (21.99)$$

with initial data  $\mathbf{M}_0 = (1 \ 0 \ 0 \ 0 \ 0 \ 0 \ 0 \ 0)^T$ .

We use the reconstructed 3-D lines listed in Tab. 21.1 to estimate the relative motion of the sample object. The results are shown in Fig. 21.16, which

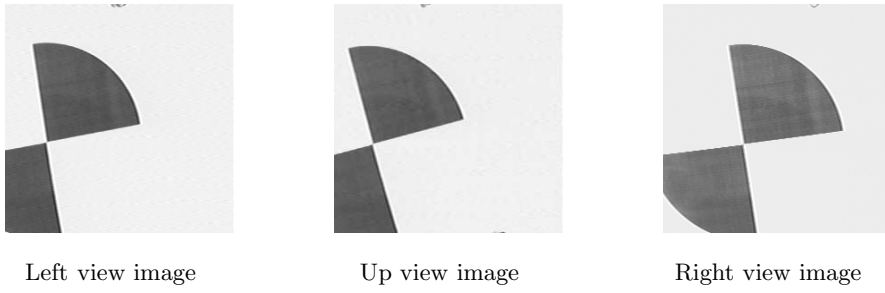


**Fig. 21.12.** A stereo triplet of a sample object at time  $i = 0$

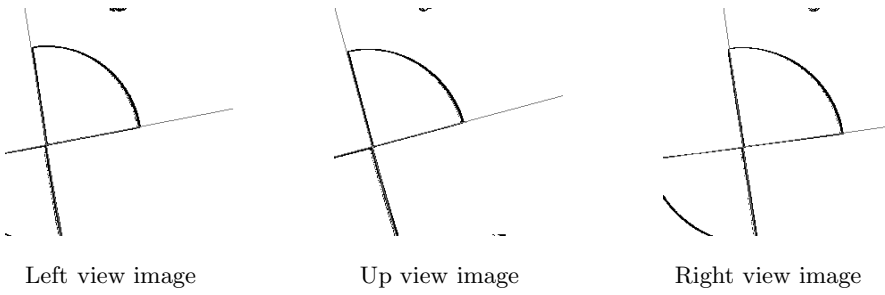


**Fig. 21.13.** Edge images of Fig. 21.12 overlapped by extracted 2-D lines

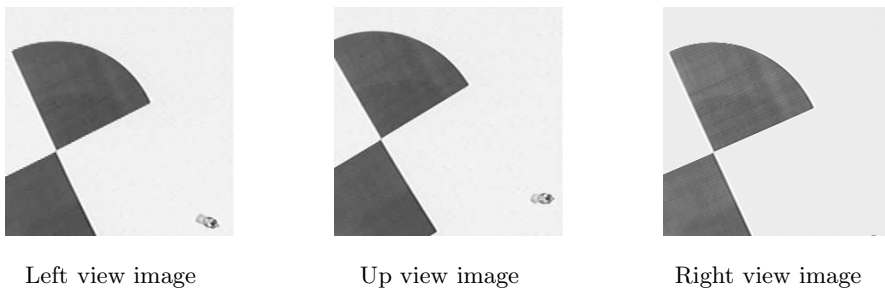


**Fig. 21.14.** A stereo triplet of a sample object at time  $i = 4$

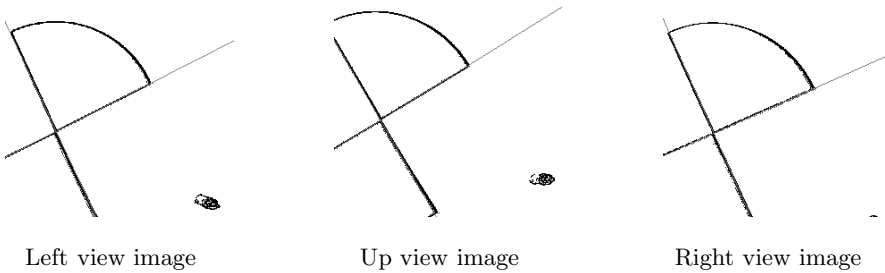


**Fig. 21.15.** Edge images of Fig. 21.14 overlapped by extracted 2-D lines

**Table 21.1.** Reconstructed 3-D lines

Time	Line item	A point on the line	direction
0	1	(0.000 3.087 -2.327)	(-0.345 0.937 -0.027)
	2	(0.556 0.000 -2.250)	(0.941 0.336 0.023)
1	1	(1.125 0.000 -2.027)	(-0.404 0.914 0.013)
	2	(0.701 0.000 -2.049)	(0.915 0.401 0.029)
2	1	(1.111 0.000 -1.82)	(-0.462 0.886 0.017)
	2	(0.794 0.000 -1.83)	(0.880 0.471 0.055)
⋮			
14	1	(0.018 0.000 0.648)	(-0.971 0.236 -0.036)
	2	(1.103 0.000 0.538)	(0.241 0.965 0.103)
15	1	(-0.680 0.000 0.753)	(-0.986 0.159 -0.025)
	2	(0.000 -6.341 0.783)	(0.171 0.985 -0.003)

shows the trajectories of eight components of the estimated motor trajectories  $\hat{\mathbf{M}}_i$  (star-solid lines) and the given motor trajectories  $\mathbf{M}_i$  (solid lines). Although we use an inaccurate initial predicted motor for the algorithm, after three or four time steps the estimations approach the truth and follow the given trajectories very well.

## 21.6 Conclusion

In this paper, we presented a new MEKF algorithm based on motor algebra to estimate 3-D motion parameters from line observations. Using motor algebra, we modeled in the 4-D space the motion of lines and the dynamic motion system. This kind of modeling linearizes the 3-D Euclidean rigid motion transformation and describes the discrete dynamic system straightforwardly.

The MEKF has the virtue that it can estimate the motion parameters from Plücker line observations. Since all recursive algorithms of the literature estimate motion parameters from observations of points or line segments with its middle point, we can claim that the use of Plücker lines is one of the most important advantages of the MEKF. Additionally, using the modeling of the lines in the motor algebra, we could linearize the nonlinear measurement model which does not face singularities, this was also a big problem of many researchers who tried in some way to apply the Kalman filter using Plücker line observations.

We first introduced the Kalman filter techniques and then presented the measurement model based on motor algebra and its constraints. This mea-

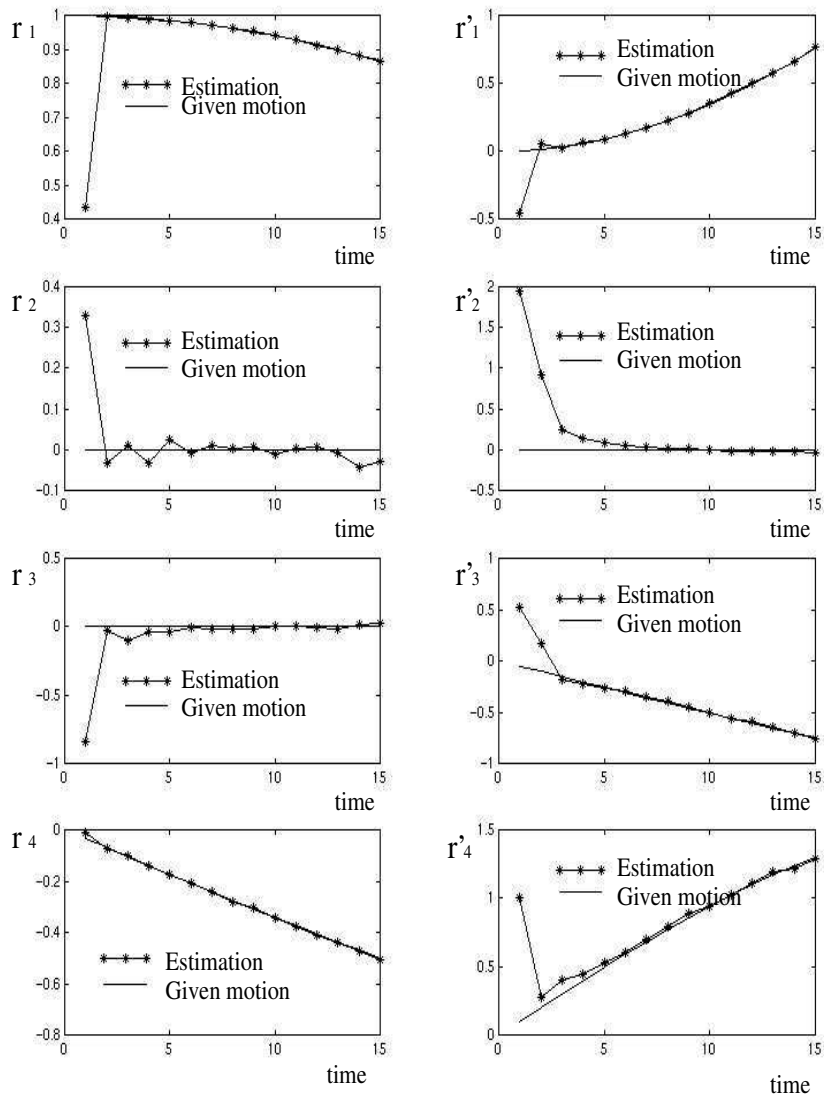


**Fig. 21.16.** The estimation results of the motor parameters by MEKF in real experiment

surement model was then linearized for Kalman filtering. We also described the dynamic motion model using motors as states from which we observe that the motor algebra is useful to effectively formulate and to compute the screw motion of a line as minimal rigid entity. In the algorithm of MEKF, we modified the estimation to satisfy the constraints, which made the estimation converge to a proper motor state.

Tests with both simulated data and real experimental data showed that the MEKF algorithm is effective to dynamically estimate the motion parameters from Plücker line observations. We also compared the MEKF with an analytical solution using least squares and the results show that the MEKF gives more accurate and more stable estimations.